Limited Amounts of Dendritic Cells Migrate into the T-Cell Area of Lymph Nodes but Have High Immune Activating Potential in Melanoma Patients

Pauline Verdijk,[1] Erik H.J.G. Aarntzen,[1,2] W. Joost Lesterhuis,[2] A.C. Inge Boullart,[1,2] Ellemieke Kok,[1] Michelle M. van Rossum,[3] Simon Strijk,[4] Femke Eijckeler,[5] Johannes J. Bonenkamp,[6] Joannes F.M. Jacobs,[1] Willeke Blokx,[5] J. Han J.M. van Krieken,[5] Irma Joosten,[7] Otto C. Boerman,[8] Wim J.G. Oyen,[8] Gosse Adema,[1] Cornelis J.A. Punt,[2] Carl G. Figdor,[1] and I. Jolanda M. de Vries[1,2,9]

Abstract

Purpose: The success of immunotherapy with dendritic cells (DC) to treat cancer is dependent on effective migration to the lymph nodes and subsequent activation of antigen-specific T cells. In this study, we investigated the fate of DC after intradermal (i.d.) or intranodal (i.n.) administration and the consequences for the immune activating potential of DC vaccines in melanoma patients.

Experimental Design: DC were i.d. or i.n. administered to 25 patients with metastatic melanoma scheduled for regional lymph node resection. To track DC *in vivo* with scintigraphic imaging and in lymph nodes by immunohistochemistry, cells were labeled with both [^{111}In]-indium and superparamagnetic iron oxide.

Results: After i.d. injection, maximally 4% of the DC reached the draining lymph nodes. When correctly delivered, all DC were delivered to one or more lymph nodes after i.n. injection. Independent of the route of administration, large numbers of DC remained at the injection site, lost viability, and were cleared by infiltrating CD163+ macrophages within 48 hours. Interestingly, 87 $\pm$ 10% of the surviving DC preferentially migrated into the T-cell areas, where they induced antigen-specific T-cell responses. Even though more DC reached the T-cell areas, i.n. injection of DC induced similar antigen-specific immune responses as i.d. injection. Immune responses were already induced with $<5 \times 10^5$ DC migrating into the T-cell areas.

Conclusions: Monocyte-derived DC have high immune activating potential irrespective of the route of vaccination. Limited numbers of DC in the draining lymph nodes are sufficient to induce antigen-specific immunologic responses.

In cancer patients, the immune system has not been able to establish an effective immune response against the tumor. Immunotherapy aims at educating the immune system to generate effective tumor-specific immune responses. Dendritic cells (DC) are specialized antigen-presenting cells that can induce *de novo* antitumor responses and are excellent candidates for cell-based immunotherapy. Whereas many DC-based clinical studies for the treatment of cancer have shown the feasibility and safety of DC vaccinations (reviewed in refs. 1, 2), the clinical efficacy of the therapy still needs to be improved (3). One important factor that determines the outcome of DC therapy is the delivery of the vaccine to immune-reactive sites, such as lymph nodes, and, more specifically, to the T-cell rich area, the paracortex. To exert their action, DC must closely encounter and interact with T cells. In addition, it has now been generally accepted that the site at which T-cell priming occurs significantly influences the homing characteristics of the effector cells (4–8). Therefore, the route of administration may be of crucial importance. It might be beneficial to combine different routes of administration; for example, in mice metastatic-like lung lesions were controlled by i.v. immunization and only partially by s.c. immunization (6). However, because DC migration to lymph nodes is very poor after i.v. injection (4), we study here only the intradermal (i.d.) and intranodal (i.n.) route. Currently, for treatment of solid tumors, the i.d. or s.c. administration of DC is most frequently used (91 clinical trials), followed by i.v. (47 trials) and i.n. (9 trials) injection (www.mmri.mater.org.au).

Authors' Affiliations: Departments of [1]Tumor Immunology, [2]Medical Oncology, [3]Dermatology, [4]Radiology, [5]Pathology, [6]Surgery, [7]Bloodtransfusion and Transplantation Immunology, [8]Nuclear Medicine, and [9]Pediatric Hemato-Oncology, Nijmegen Centre for Molecular Life Science, Radboud University Nijmegen Medical Centre, Nijmegen, The Netherlands

Received 10/21/08; revised 12/15/08; accepted 12/15/08; published OnlineFirst 3/24/09.

Grant support: Dutch Cancer Society grants KUN 99/1950, KWF 2003-2918, KWF 2004-3126, and KWF 2004-3127; the Netherlands Organization for Scientific Research grant 920-03-250 (W.J. Lesterhuis); the Tumor Immunology Lab Foundation; the Nijmeegs Offensief Tegen Kanker-foundation; NIH RO1 grant NS045062; and the European Union projects Cancer Immunotherapy and DC-THERA.

The costs of publication of this article were defrayed in part by the payment of page charges. This article must therefore be hereby marked *advertisement* in accordance with 18 U.S.C. Section 1734 solely to indicate this fact.

Requests for reprints: I. Jolanda M. de Vries, Department of Tumor Immunology, Radboud University Nijmegen Medical Centre, P.O. Box 9101, 6500 HB Nijmegen, The Netherlands. Phone: 31-24-3617600; Fax: 31-24-3540339; E-mail: j.devries@ncmls.ru.nl.

doi:10.1158/1078-0432.CCR-08-2729

Translational Relevance

This article describes an already clinically applied vaccination strategy. The data described here will be instrumental for optimizing this strategy with antigen-loaded dendritic cells.

Scintigraphic imaging of cancer patients injected with DC labeled with [^{111}In]-indium or [^{99m}Tc]-technetium showed that only after i.d. or s.c. (9–16), i.n. (9, 11, 17), and intralymphatic (11, 18) injection did DC migrate to the draining lymph node regions. More substantial evidence was obtained in our previous study, in which DC were labeled with both ^{111}In and paramagnetic iron oxide particles (SPIO), which is a suitable contrast agent for magnetic resonance imaging (17). We showed that after i.n. injection, DC were indeed present in the injected node and had migrated to nearby lymph nodes. However, these images do not show how many cells actually reach the T-cell area and provide no information on the phenotype and quality of the injected cells and whether the label is still present in the administered cells. SPIO-labeled DC can be easily visualized in resected lymph nodes and allow a detailed analysis of the fate and local immune effects of the injected DC in the targeted lymph nodes. We show that, although the majority of nonmigrating DC at the injection site are phagocytosed by macrophages, part of the SPIO-labeled cells migrate into the T-cell areas, exhibit a DC phenotype, and activate specific T cells. Because the immune responses in both groups of patients were comparable, there was no advantage of i.n. injection over i.d. administration.

Patients, Materials, and Methods

Patients. Eligibility criteria included stage III and IV melanoma according to the American Joint Committee on Cancer criteria (19), HLA-A2.1 phenotype, and melanoma expressing the melanocyte-associated antigens gp100 and tyrosinase. The study was approved by our Institutional Review Board, and written informed consent was obtained from all patients.

Treatment schedule. At day -7, peripheral blood mononuclear cells (PBMC) were obtained by leukapheresis for DC culturing. DC loaded with both keyhole limpet hemocyanin (KLH) and tumor-associated antigen (TAA) peptides were injected either i.n. into a lymph node of the region that was to be resected or i.d. in close vicinity of this lymph node region. On day 0, patients received either an i.n. injection of ^{111}In-labeled DC (7.5×10^6) mixed with SPIO-labeled DC (7.5×10^6; total volume 100 μL) directly into a lymph node or an i.d. injection of DC labeled with both ^{111}In and SPIO (15×10^6; total volume 100 μL). I.n. injections were done under ultrasound guidance by an experienced radiologist. Scintigraphic imaging of the lymph node region was done 30 min after i.n. injection, and 24, 48, and/or 48 h after i.n. or i.d. injection, before dissection of the regional lymph nodes. Two patients received an i.n. injection in both the left and the right lymph node region.

Radiolabeled lymph nodes were dissected from the surgical specimen under the guidance of a γ-probe (Europrobe; Eurorad) and then fixed in Unifix (Klinipath). The lymph nodes were embedded in paraffin and were processed for histology and immunohistochemistry. Patients received three more vaccinations at days 14, 28, and 42.

DC culture and labeling. DC were generated from adherent PBMC by culturing in the presence of interleukin 4 (500 U/mL) and granulocyte-monocyte colony-stimulating factor (800 U/mL; both Cellgenix). On day 4, DC were loaded with the control antigen KLH (10 μg/mL; Calbiochem) and were labeled with SPIO by adding 100 μg Ferumoxide/mL (Endorem; Laboratoire Guerbet) 3 d after the onset of DC culturing (17). On day 5, DC were matured with autologous monocyte-conditioned medium supplemented with prostaglandin E_2 (10 μg/mL; Pharmacia & Upjohn) and 10 ng/mL recombinant tumor necrosis factor-α (Cellgenix) for 48 h as described previously (20, 21). After maturation, 60 ± 23% of the SPIO DC and 77 ± 17% of unlabeled DC expressed high levels of CD83, and <10 ± 8% of all DC expressed residual levels of CD14, analyzed by fluorescence-activated cell sorting analysis as described below. DC were pulsed with the melanoma peptides gp100:154-167, gp100:280-288, and tyrosinase:369-376 as described previously (9). Mature DC were labeled with ^{111}In-oxine (Covidien) in 0.1 mol/L Tris-HCl (pH 7.0) for 15 min at room temperature as described previously (9, 20), resulting in 4 MBq activity per 7.5×10^6 cells.

Scintigraphic imaging. *In vivo* and *ex vivo* planar scintigraphic images (256×256 matrix, 174 and 247 keV ^{111}In photopeaks with 15% energy window) of the injection depot and the corresponding lymph node basin were acquired with a γ-camera (Siemens ECAM) equipped with medium energy collimators at day 0 and day 2. Migration was quantified by region of interest analysis of the individual nodes visualized on the images and expressed as the relative fraction of ^{111}In-labeled DC that had migrated from the injection depot to successive lymph nodes after 2 d.

Iron staining and immunohistochemistry of histopathologic sections. Sections (5 μm) of the resected radiolabeled lymph nodes were stained with H&E or with Prussian blue to detect SPIO-labeled cells. Slides were stained with 2% potassium hexacyanoferrate (II)-trihydrate in 0.2 mol/L HCl for 15 min and were counterstained with 0.05% nuclear fast red in 5% aluminum sulphate. Immunohistochemical stainings were done on paraffin-embedded tissue sections with the use of monoclonal antibodies. Paraffin sections were dewaxed and rehydrated. All reactions were done at room temperature unless stated otherwise. Endogenous peroxidase activity was blocked by incubation in PBS containing 3% H_2O_2 for 30 min. After rinsing with PBS, antigen retrieval consisted of microwave boiling in either 10 mmol/L sodium citrate buffer (pH 6.0) or 10 mmol/L EDTA/1 mmol/L Tris buffer (pH 8.0 or 9.0) for 10 min, depending on the primary antibody. After boiling, slides were allowed to cool down for at least 2 h. After rinsing with PBS, slides were pretreated with 20% normal horse serum for 10 min to reduce nonspecific staining. All sera and antibodies were dissolved in PBS with 1% bovine serum albumin. Subsequently, slides were incubated in a humidity chamber with the primary antibody at 4°C for 16 to 20 h. The following primary monoclonal antibodies were used: CD4, CD8 (both from Beckman Coulter), CD25, CD69, CD83, and CD163 (Novocastra). The avidin-biotin complex (Vector) method was used for visualization with 3,3′-diaminobenzidine hydrochloride solution. Staining of the 3,3′-diaminobenzidine substrate was intensified with a 0.5% copper sulfate solution. Slides were counterstained with hematoxylin solution or nuclear fast red. Sections were analyzed by microscopy (Zeiss Axioskop 2 plus; Zeiss or Leica DMLB microscope; Leica) with the use of ProgRes CapturePro (Jenoptik) or Leica IM500 (Leica) software.

Humoral responses to KLH. Antibodies against KLH were measured in the serum of vaccinated patients by ELISA (22). Microtiter plates (96 wells) were coated overnight at 4°C with KLH (25 μg/mL in PBS per well). After washing the plates, different concentrations of patient serum (range, 1 in 100 to 1 in 500,000) were added for 1 h at room temperature. After extensive washing, specific antibodies[Q_: Correct expanded form of Ab?] (total IgG, IgG1, IgG2, and IgG4) labeled with horseradish peroxidase were allowed to bind for 1 h at room temperature. Peroxidase activity was revealed with the use of 3,3′5,5-tetramethyl-benzidine as substrate and was measured in a microtiter plate reader at 450 nm.

Proliferation assay. Cellular responses against KLH were measured in a proliferation assay. Briefly, PBMC isolated from blood samples taken

before each DC vaccination were plated in a 96-well tissue culture microplate with or without KLH. After 4 d of culture, 1 μCi per well of tritiated thymidine was added for 8 h, and incorporation of tritiated thymidine was measured in a β-counter.

Isolation of lymph node DC and T cells. Cell suspensions were made from resected radiolabeled lymph nodes from three patients. Lymph node tissue was cut into small fragments in Hanks Balanced Salt Solution medium (GIBCO) with 50 μg/mL collagenase type 1A, 10 μg/mL DNase, and 1 μg/mL trypsin inhibitor (Sigma Chemical Co.). The fragments were incubated for 30 min at 37°C. For the isolation of DC–T cell rosettes, the large fragments were left to settle down, and the supernatant was transferred to a fresh tube. SPIO-containing DC were isolated with the use of a Dynal MPC magnet. Cells were washed with RPMI supplemented with 7% human serum. The isolated SPIO DC were spun onto microscope slides and were stained with H&E. From two patients, lymph node cells were cultured for 4 to 6 wk in RPMI/7% human serum and 200 IU/mL of interleukin 2. KLH-specific T-cell proliferation was measured in a proliferation assay. Fresh autologous PBMC were loaded with KLH overnight, irradiated, and used as stimulator cells for lymph node T cells (ratio, 1:1). After 4 d of culture, 1 μCi per well of tritiated thymidine was added for 8 h, and incorporation of tritiated thymidine was measured in a β-counter.

Delayed-type hypersensitivity. One to 2 wk after the four DC vaccinations, a delayed-type hypersensitivity (DTH) skin test was done. Briefly, DC pulsed with peptides and DC pulsed with peptides plus KLH (2×10^5 DC each) were injected i.d. into the skin of the back of the patients at four different sites. The diameter (in millimeters) of induration was measured after 48 h, and punch biopsies (6 mm) were obtained under local anesthesia. Biopsies were cut in half; one part was frozen directly in liquid nitrogen for immunohistochemistry, and the other part was cut into small pieces and cultured in RPMI/7% human serum supplemented with interleukin 2 (100 U/mL). Every 7 d, half of the medium was replaced by fresh interleukin 2–containing RPMI/7% human serum. After 2 to 4 wk of culturing, the T cells were tested for antigen recognition or tested for tetramer binding. For tetramer binding, the PBMC of T cells were incubated with allophycocyanin-labeled tetrameric MHC containing the gp100:154-167, gp100:280-288, or tyrosinase:369-376 peptide (Sanquin) for 1 h, and then were washed and analyzed by flow cytometry.

Antigen-recognition assay. Antigen recognition was determined by the production of cytokines by DTH-derived cells in response to T2 cells pulsed with the indicated peptides or BLM (a melanoma cell line expressing HLA-A2.1 and with no endogenous expression of gp100 and tyrosinase), transfected with control antigen G250, or with gp100 or an allogenic HLA-A2.1–positive, gp100-positive, and tyrosinase-positive tumor cell line (MEL624). Cytokine production was measured in supernatants after 16 h of coculture by the cytometric bead array (Th1/Th2 Cytokine CBA 1; BD Pharmingen).

Statistics. Data were analyzed with the use of unpaired Student's *t* test; *P* values <0.05 were considered to be statistically significant.

Results

Biodistribution of ^{111}In/SPIO DC after i.d. and i.n. vaccination. To study the distribution of the DC vaccine after i.d. and i.n

Table 1. Overview of patients and results

I.d.	% distant from injection site	Lymph nodes available	Injection site available	KLH-specific PBMC*	KLH-specific antibodies	DTH tetramer$^+$ T cells	IFN-γ–producing DTH T cells
ID01	3.7	+	-	+	+	-	+
ID02	0.8	+	-	+	+	+	+
ID03	0.1	-	+	+	+	-	nd
ID04	0.3	+	-	++	+	-	-
ID05	0.3	+	-	++	+	-	-
ID06	0.8	-	+	++	†	+	+
ID07	0.6	-	-	++	nd	-	-
ID08	0.5	-	+	++	+	-	-
ID09	2.6	+	-	+	+	-	-
ID10	1.8	+	-	++	+	+	-
ID11	0.8	+	+	‡			
ID12	1.6	+	-	+	+	+	+
Total		8	4	11 of 11	9 of 10	4 of 11	4 of 10
I.n.							
IN01	40	+	+	++	+	+	-
IN02	0	+	-	+++	+	-	-
IN03	0	§	-	+	-	-	nd
IN04	0	§	-	+	+	nd	nd
IN05	4 / 2	+	+	+++	+	+	+
IN06	26	+	-	++	+	+	+
IN07	0 / 1	§	-	+++	-	-	nd
IN08	0	§	-	++	+	-	-
IN09	1	+	+	+++	+	-	nd
IN10	7	+	+	+	nd	‡	
IN11	0	+	+	++	+	+	-
IN12	22	+	+	+++	+	+	+
IN13	56	+	+	++	+	+	+
Total		9	7 of 9	13 of 13	10 of 12	6 of 11	4 of 8

Abbreviation: nd, no data.
*Maximal proliferation index: +, 3 to 10, ++, 10 to 30, +++, >30.
†KLH-binding antibodies present before vaccination.
‡Progressive disease during treatment; treatment was stopped.
§Lymph node missed during injection; determined by magnetic resonance imaging, De Vries et al. (17).

injection in patients with metastatic melanoma, DC were labeled with ^{111}In and SPIO for the first vaccination and injected in (the vicinity of) a lymph node region 24 to 72 hours before scheduled lymph node resection. Delivery of the DC to skin-draining lymph nodes after i.d. (n = 12) and i.n. injection (n = 13) was monitored by scintigraphic imaging of the lymph node region (Table 1). After i.d. administration, never >4% migration was observed (Fig. 1A; mean, 1.1 ± 1.1%). In contrast, the percentage of cells reaching nearby lymph nodes after i.n. administration was highly variable and ranged from 0% to 56% (Fig. 1B; mean, 10.6 ± 17.5%). In five patients, distribution to more than one lymph node had already taken place within the first 30 minutes after injection, indicating that DC had spread via the lymphatic system during injection. Migration to subsequent lymph nodes increased in the next 24 to 72 hours. In six patients, DC remained localized at the injection site, suggesting that either DC had not (detectably) migrated or that DC were not correctly injected into a lymph node. For five patients, the latter was indeed confirmed with magnetic resonance imaging as previously described (17). In the resected lymph node basin from the sixth patient, an ^{111}In-positive lymph node was isolated, showing that the injection was correct but that the cells had not migrated to nearby lymph nodes. Taken together, although maximally 4% of the DC reached the draining lymph nodes after i.d. injection, all DC were delivered to one or more lymph nodes after i.n. injection when correctly delivered.

Numerous ^{111}In/SPIO DC die at the injection site and are phagocytosed by macrophages. Because the presence of ^{111}In/SPIO DC inside lymph nodes does not necessarily imply that DC actually reach the T-cell area, we analyzed the dissected radiolabeled lymph nodes by immunohistochemistry to visualize ^{111}In/SPIO DC. Lymph nodes were obtained from eight and nine patients that received i.d. or i.n injections, respectively. In addition, biopsies from the i.d. injection site were obtained and analyzed in the same way. Although single ^{111}In/SPIO DC were present in the sinuses and paracortex of draining lymph nodes, a large depot of SPIO$^+$ cells was found at the site of injection, as was expected from the scintigraphs. This was not only observed after i.d. vaccination (Fig. 1C) but also after i.n. injection (Fig. 1D). In lymph nodes from patients in which immediate redistribution of the DC after injection was observed, ^{111}In/SPIO DC also accumulated in the sinuses of subsequent nodes (not shown).

To verify whether the SPIO$^+$ cells at the i.d. or i.n. injection site were indeed DC and not phagocytes that have taken up label, lymph node sections were stained for the DC marker CD83 and for the macrophage marker CD163 (23). This revealed that in the dermis, only part of the SPIO$^+$ cells in the injection site expressed CD83 (Fig. 2A). In the CD83-negative

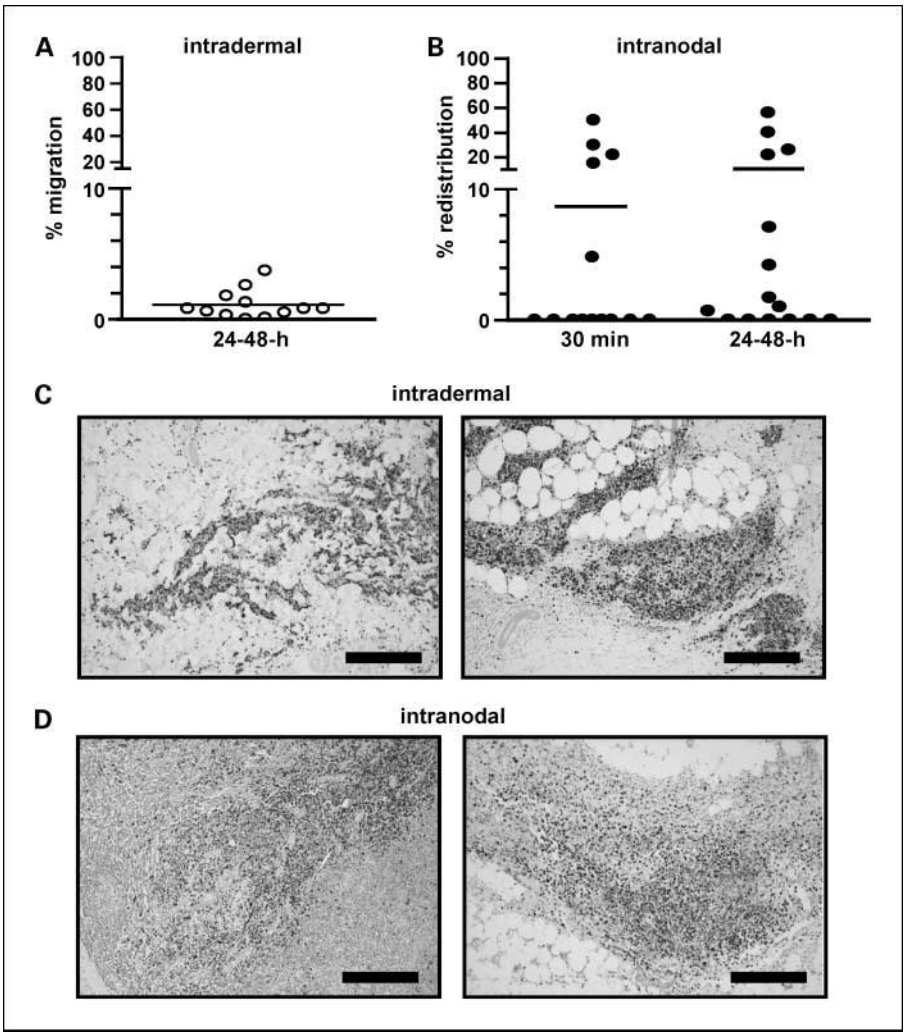

Fig. 1. ^{111}In/SPIO DC migrate to lymph nodes, but most remain at site of injection. Melanoma patients received i.d. or i.n. injections of ^{111}In-labeled and SPIO-labeled DC 48 h before surgery. *A* to *B,* percentage of cells redistributed to nearby lymph nodes after i.d. (*A*) and i.n. (*B*) injection of ^{111}In-labeled and SPIO-labeled DC imaged by scintigraphy of the lymph node region. Symbol, one injection of 15 × 10^6 cells (*open symbol*, i.d.; *closed symbol*, i.n.); line, mean redistribution. Migration of radiolabeled DC was measured 30 min and/or 24 to 48 h after injection. *C* to *D,* resected lymph nodes and skin biopsies were analyzed for the presence of SPIO-labeled cells by Prussian blue staining. *C,* injection site in the dermis after i.d. vaccination (two patients; ×50). *D,* injection site in the lymph node after i.n. vaccination (two patients; ×50). Bar, 500 μm.

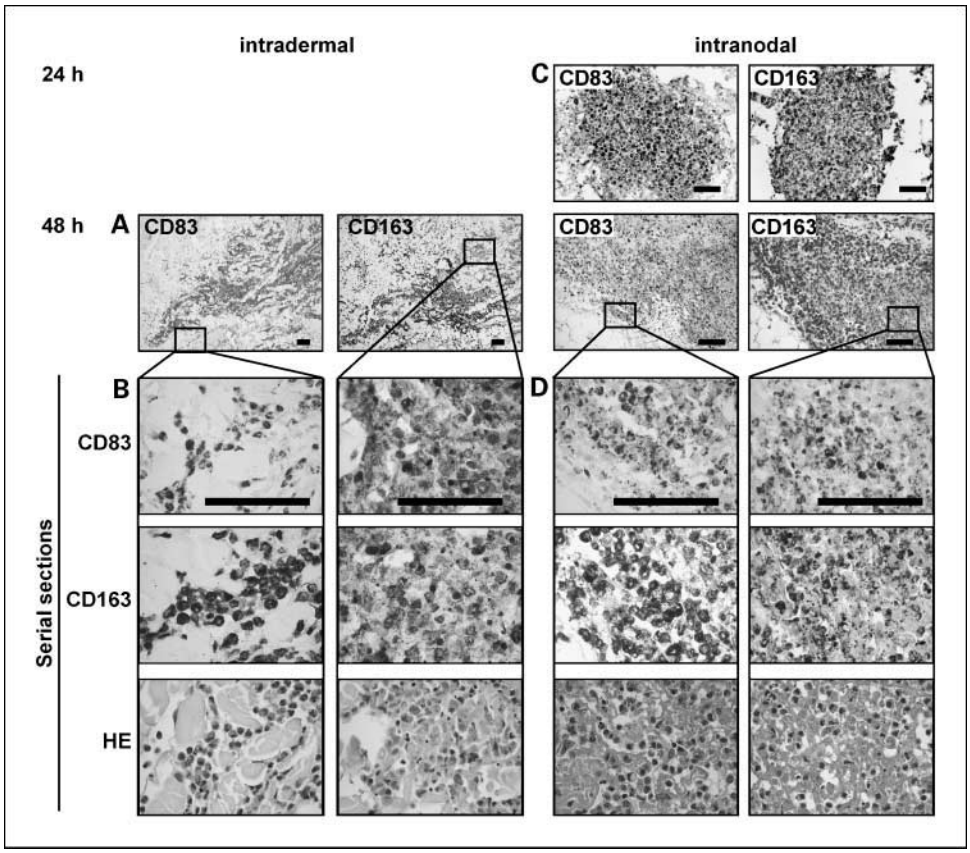

Fig. 2. Expression of DC and macrophage markers on SPIO$^+$ cells in the injection depot. Paraffin-embedded sections of i.d. (*A* and *B*) and i.n. (*C* and *D*) injection sites were stained with H&E or with antibodies for CD83 and CD163. *A,* overview of CD83 (*left*) and CD163 (*right*) expression in injection site 48 h after i.d. injection of ^{111}In/SPIO DC (×50). *C,* overview of CD83 (*left*) and CD163 (*right*) expression in injection site in lymph nodes resected 24 h (*top*) or 48 h (*bottom*) after injection of ^{111}In/SPIO DC (×100). *B* and *D,* higher magnification (×400) of indicated areas in *A* and *B*, stained for CD83, CD163, or with H&E (×400). Bar, 100 μm. In H&E stainings, SPIO is visible as brown granula. In immunostainings, SPIO was visualized by Prussian blue staining, and nuclei were stained with nuclear fast red.

areas, all SPIO$^+$ cells were positive for the macrophage marker CD163 (Fig. 2A and B). Staining with H&E revealed that in areas with the most CD83$^+$ ^{111}In/SPIO DC, cells were enlarged and exhibited pale-pink nuclei, typical for necrotic cells. At the same time, the SPIO$^+$ cells in the CD163$^+$ area seemed viable, exhibiting regular hematoxylin staining of the nuclei (Fig. 2B), suggesting that macrophages had infiltrated the injection site and had phagocytosed dead ^{111}In/SPIO DC. Comparable results were found after i.n. injection (Fig. 2C and D). Most of the SPIO$^+$ cells at the site of injection still expressed CD83 at 24 hours (one patient), but numerous small macrophages containing no or little SPIO were present in between enlarged SPIO$^+$ cells (Fig. 2C, *top*). In lymph nodes resected after 48 hours, CD83 expression was rare and was mainly found in the center of the depot, whereas macrophages were present throughout the injection site (Fig. 2C, *bottom*, and D). As in i.d. injection sites, necrotic cells were found at sites where CD83 expression was most abundant, whereas in areas with only CD83$^-$ SPIO$^+$ macrophages, cells seemed viable. Thus, the majority of the ^{111}In/SPIO DC remained at the injection site and had lost viability, whereas macrophages infiltrated the depot and phagocytosed dead ^{111}In/SPIO DC.

^{111}In/SPIO DC migrate into the T-cell areas and activate antigen-specific T cells. Although most ^{111}In/SPIO DC were trapped at the site of injection, single SPIO$^+$ cells were found scattered in draining lymph nodes both after i.d. injection and in the injected and subsequent nodes after i.n. injection. We evaluated the CD83 expression and location within the lymph node of these SPIO$^+$ cells. After i.d. injection, SPIO$^+$ cells can only reach the draining lymph nodes by active migration via the afferent lymphatics. Indeed, SPIO$^+$ cells were predominantly found in the T-cell areas (93 ± 9%) and sometimes in the subcapsular sinuses (Fig. 3A, *left*). Of all the SPIO$^+$ cells in the paracortex, 85 ± 13% were CD83$^+$ DC (Fig. 3B), indicating that mainly viable ^{111}In/SPIO DC and only a few SPIO$^+$ macrophages had migrated to the draining lymph nodes and into the T-cell areas.

After i.n. injection, more SPIO$^+$ cells were dispersed over the lymph nodes than after injection in the dermis. SPIO$^+$ cells were present in high numbers both in the sinuses and the paracortex. We estimated the total number of SPIO$^+$ cells in the paracortex in single lymph node sections after i.n. injection to be 10-fold to 30-fold higher than after i.d. administration. However, many SPIO$^+$ macrophages were also present both in the injected node and in nearby lymph nodes. Analysis of the paracortex of all lymph nodes revealed that 54 ± 21% of all SPIO$^+$ cells in the paracortex were DC. Within each section, the ratio between ^{111}In/SPIO DC and SPIO$^+$ macrophages was variable and correlated with the distance from the depot. In close vicinity of the injection depot, 5% of the SPIO$^+$ cells were CD83$^+$ ^{111}In/SPIO DC, whereas at more distant sites, virtually all of the SPIO$^+$ cells expressed CD83 (not shown). Quantitative analysis of the total number of SPIO$^+$ cells was only possible in sections of the lymph nodes where DC had migrated to. Quantification of CD83$^+$ and CD163$^+$ expression revealed that only 35 ± 26% of all SPIO$^+$ cells were CD83$^+$ DC (Fig. 3A, *right*, and C). Interestingly, 87 ± 10% of these CD83$^+$ ^{111}In/SPIO DC were found in the T-cell area, indicating that ^{111}In/SPIO DC that do survive preferentially migrate into the paracortex.

DC in T-cell area are fully functional and activate T cells. We next analyzed whether ^{111}In/SPIO DC that had migrated into

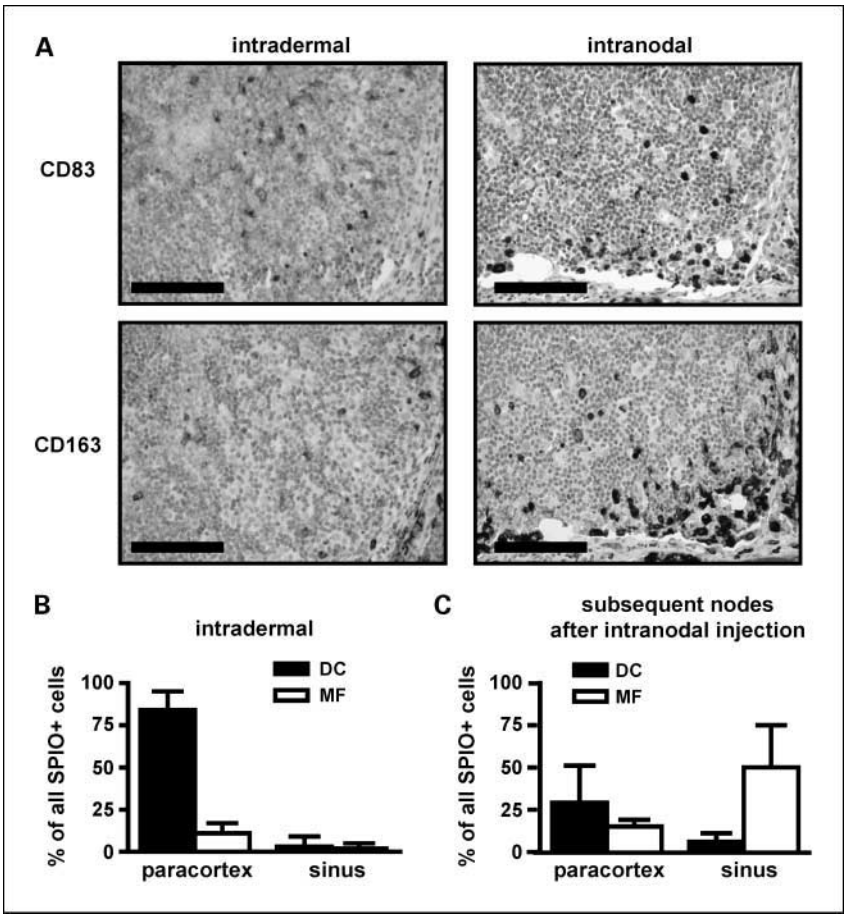

Fig. 3. ^{111}In/SPIO DC preferentially migrate into the T-cell area. Immunohistochemistry of paraffin-embedded sections of lymph nodes to which DC had migrated after i.d. and i.n. injection. *A,* T-cell area of lymph nodes after i.d. (*left*) and i.n. (*right*) stained for CD83 and CD163 (×200). *B* and *C,* graphs representing the percentage of SPIO$^+$ cells expressing CD83 or CD163 in the paracortex and sinuses of draining lymph nodes after i.d. injection (*B*) and of lymph nodes after i.n. injection that do not contain injection depots (*C*). Bar, 100 μm.

the paracortex of the (draining) lymph nodes were still functional and able to interact with resident T cells. SPIO$^+$ DC in the T-cell area colocalized with both CD4$^+$ and CD8$^+$ T cells (Fig. 4A). Interestingly, in various cells the staining for CD8 was most prominent at the interface between the T cell and the SPIO-positive cells (Fig. 4B, *second panel*). This explicit localized expression of CD8 molecules suggests that the T cells are actively engaged with the DC in a way that stimulated the redistribution of the CD8 molecules and likely the formation of an immunologic synapse. Activation of T cells surrounding the injected DC was further supported by the expression of the early T-cell activation marker CD69 and the activation marker CD25 (Fig. 4B). Of the SPIO$^+$ cells in the T-cell area, 65 ± 22% were in the immediate proximity of CD69$^+$ cells (8 lymph nodes from six patients). Similarly, 64 ± 13% of the SPIO$^+$ cells in the paracortex were surrounded by CD25$^+$ T cells (10 lymph nodes from six patients).

To further investigate the immune activating potential of the migrated ^{111}In/SPIO DC, they were isolated from a lymph node cell suspension by a magnet. We found that some of these DC were still forming rosettes with T cells (Fig. 4C). In addition, we could show that T cells cultured from lymph node suspensions of two i.n. vaccinated patients showed KLH-specific proliferation (Fig. 4D). Thus, ^{111}In/SPIO DC interacted with T cells and induced antigen-specific T cell responses within 48 hours after vaccination.

Systemic immune responses after i.d. and i.n. vaccination with DC are comparable despite difference in number of DC in T-cell area. To test whether the differences in ^{111}In/SPIO-DC distribution after vaccination by different routes of administration had any effect on the strength of immune activation, we compared the immune responses elicited in patients that received multiple injections. To monitor the capacity of vaccinated DC to initiate an immune response, DC were not only pulsed with TAA peptides but also loaded with the foreign protein KLH. We observed that most patients (i.n., 11 of 13; i.d., 10 of 11) developed an IgG antibody response against KLH after DC vaccination, with serum levels increasing after each vaccination (Fig. 5A). Levels of KLH-specific IgG antibody were comparable after i.n. and i.d. vaccination. In addition, KLH-specific proliferation of CD4$^+$ T cells was induced in all i.n. and i.d. injected patients (Fig. 5B). Thus, despite the difference in the number of DC that reach the skin-draining lymph nodes, there was no effect on the strength of the immune response against KLH after i.n. or i.d. injection.

Next we compared the capacity of i.d. and i.n. injected DC to induce specific CD8$^+$ T-cell responses against the tumor-associated peptides used for loading. TAA responses were tested by staining T cells with HLA-A2.1 tetramers encompassing gp100:154, gp100:280, or tyrosinase:369 peptides. In one patient in each group, we could already detect tetramer-specific T cells in PBMC freshly isolated after four vaccinations. Because the frequency of peptide-specific T cell in the blood is very low and often undetectable, DTH responses were induced by injecting peptide-loaded DC i.d. We have shown previously that sampling of DTH sites is a very powerful approach to

detect vaccine-related T cells (24). No significant differences were found in the number of patients with tetramer$^+$ and IFN-γ–producing T cells isolated from DTH reactions. TAA tetramer–positive T cells were found in 4 out of 11 patients after i.d. vaccination and in 6 out of 11 patients after i.n. vaccination (Table 1; example in Fig. 5C). The functionality of these T cells was tested by coculturing with T2 cells loaded with TAA peptides and measuring the IFN-γ production. Both after i.d. (4 of 10 patients) and after i.n. (4 of 8 patients), T cells from DTH biopsies produced IFN-γ in cocultures with peptide-loaded target cells (Table 1; example in Fig. 5D). Thus, despite the limited number of DC migrating to subsequent lymph nodes, immunologic responses were found in most patients, and no significant differences were found in the immunologic responses after i.n. and i.d. DC vaccination.

Discussion

Previously, we have shown that DC can be tracked *in vivo* both by scintigraphic imaging and magnetic resonance imaging (9, 17). In this study, we monitored the migration of DC into the T-cell area, the paracortex, of the lymph node at a microscopic level. Although *in vivo* imaging provided us with a lot of information on the distribution of the DC vaccine after injection, the limitation is that lymph nodes can only be generally qualified as positive for the cell-tracking label. Here we exploit immunohistochemistry to show that many DC remained at the site of injection where they died and were cleared by macrophages. Nevertheless, small numbers of labeled DC did reach the lymph node and migrated into the T-cell area, where they interacted with T cells and induced immune responses against KLH and TAA. Importantly, despite the fact that more DC reached the T-cell areas after i.n. injection, DC were equally well capable of inducing immune responses.

In vivo tracking of *ex vivo*–generated cells is an important readout for the evaluation of cellular therapy. Our results explicate that *in vivo* tracking of therapeutic cells primarily tracks the cell label and may need to be confirmed with immunohistochemical studies. For example, whereas quantification of migrated DC after i.d. injection proved to be quite accurate (~85% of the migrated cells were indeed DC),

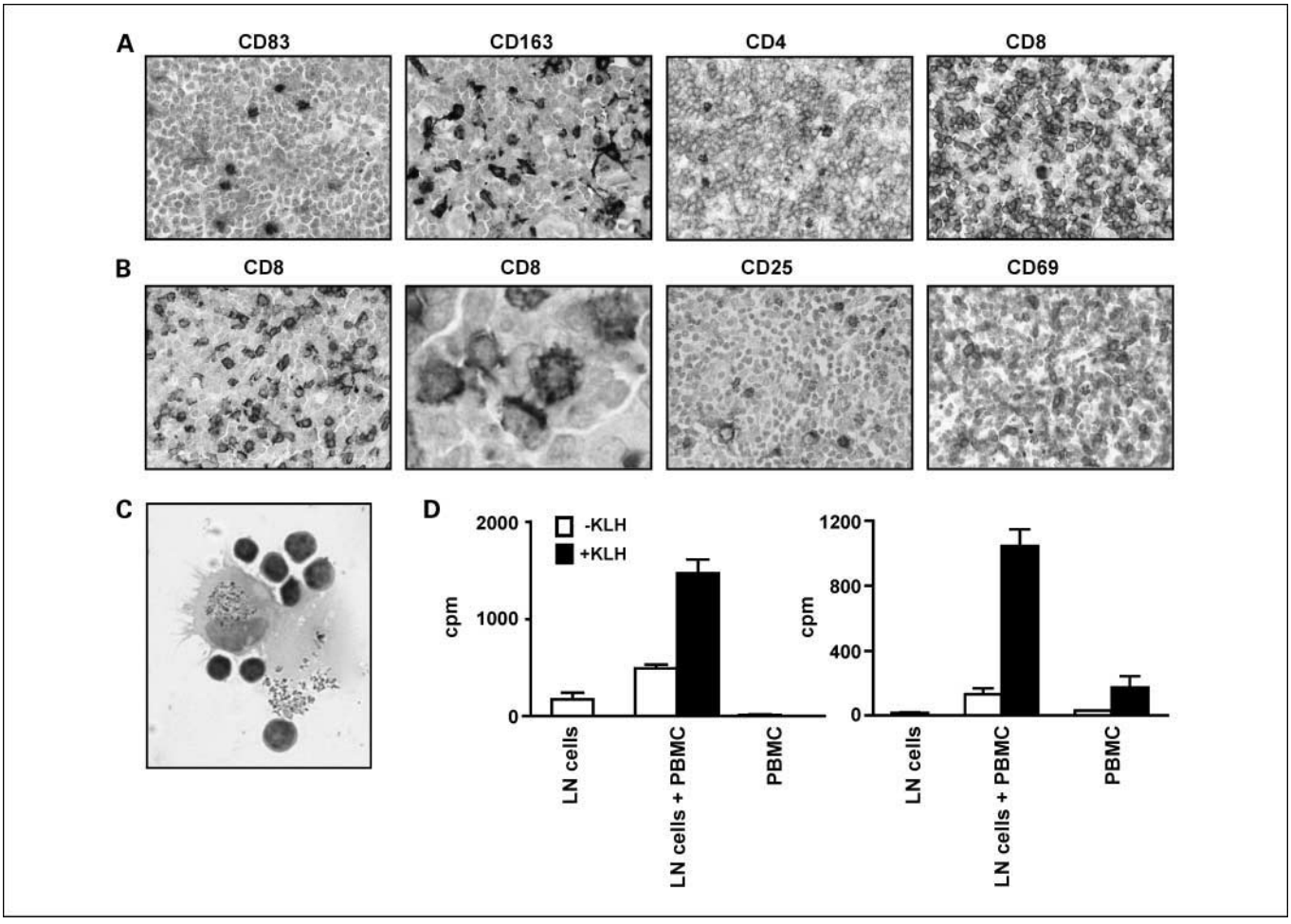

Fig. 4. ^{111}In/SPIO DC interact with lymph node T cells and activate KLH-specific T cells. *A,* T-cell area after i.n. injection stained for CD83, CD163, CD4, and CD8 (×630). Bar, 20 μm. *B,* T-cell area of lymph node after i.n. injection stained for CD8 (*second panel*, detail of first panel), CD69 (*third panel*), and CD25 (*last panel*; original magnification, ×630). Bar, 20 μm. Iron oxide was visualized by Prussian blue staining. Nuclei were stained with hematoxylin (*A* and *E, right*) or nuclear fast red (*D* and *E, left*). *C,* rosette of a SPIO-labeled DC with T cells magnetically isolated from a lymph node of a patient after i.n. injection. Bar, 20 μm. *D,* KLH-specific proliferation of lymph node–derived T cells from two patients after one i.n. DC injection. T cells were cocultured with irradiated autologous PBMC loaded with (*black bars*) or without (*white bars*) KLH. Proliferation was measured in a tritiated thymidine incorporation assay.

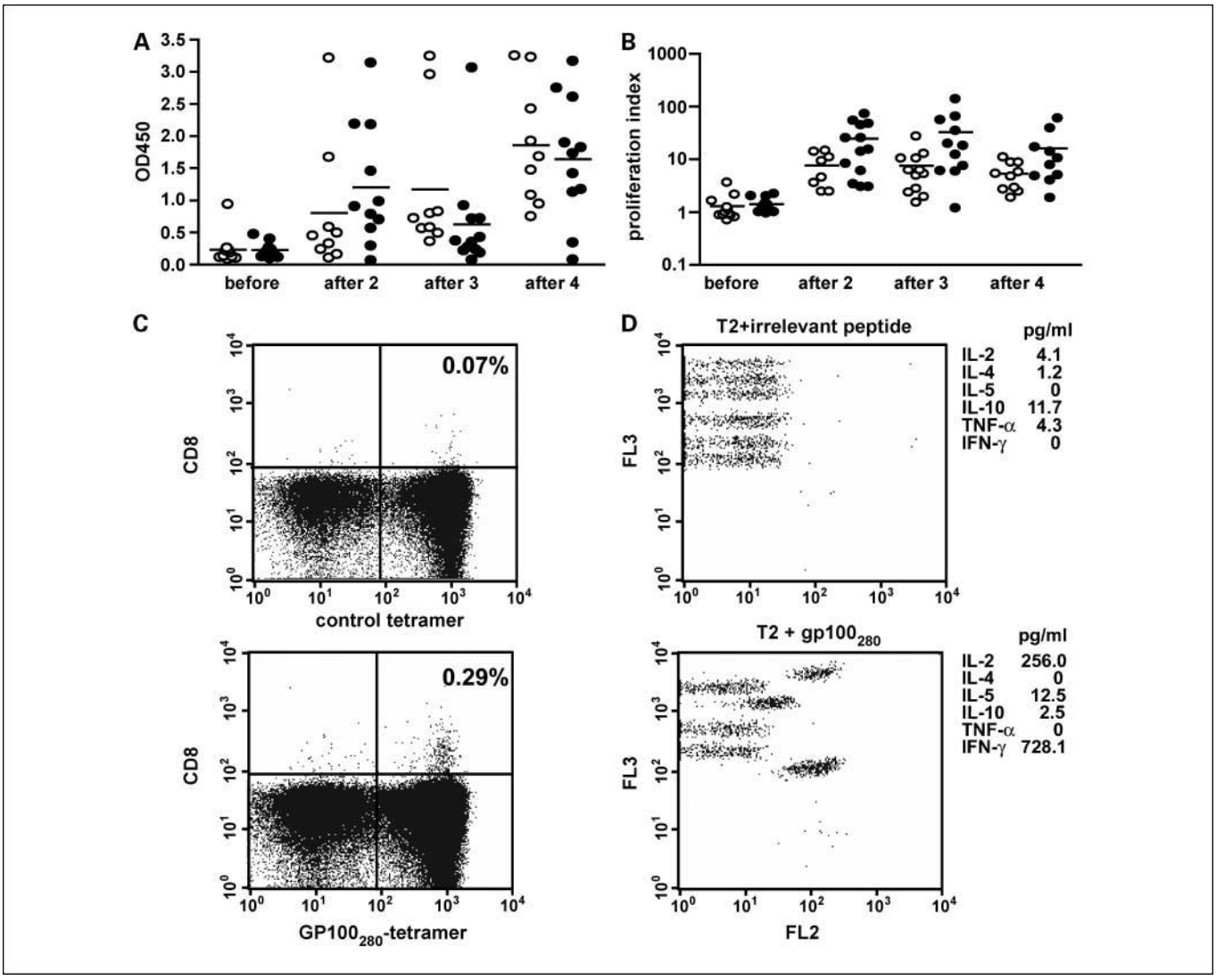

Fig. 5. Immune activation by DC vaccination. Immunologic response against KLH in the peripheral blood (*A* and *B*) and TAA peptides in DTH biopsies (*C* and *D*) of patients before and after DC vaccination. *A* and *B,* PBMC and serum were isolated from blood from vaccinated patients at days 30, 44, and 56, respectively, after two, three, and four vaccinations. Symbols, individual patient (*open circles*, i.d. vaccination; *closed circles*, i.n. vaccination); line, mean. *A,* antibody response against KLH. Graphs, OD450 values of total IgG directed to KLH in serum of individual patients diluted 1 in 200. *B,* KLH-induced proliferation of PBMC of melanoma patients before and after DC vaccination. Each symbol, one patient (*open symbols*, i.d. injections; *closed symbols*, i.n. injections); line, mean. *C,* example of tetramer staining of T cells cultured from DTH reactions from patient IN12. Cells were stained with allophycocyanin-labeled tetramers encompassing an irrelevant peptide (*left*) or the gp100:280-280 peptide (*right*) and with CD8-FITC. *D,* cytokine secretion profile of the supernatant of the same T cells. Shown is the fluorescence-activated cell sorting scatter plot of the cytokine bead array incubated with the supernatant of T cells after stimulation with T2 cells loaded with an irrelevant peptide or with the gp100:280-288 peptide.

quantification of the number of viable therapeutic cells that had actually migrated after i.n. injection was not possible because the migrated cells as well as the depot were present within the same lymph nodes. Therefore, not only viable DC but also nonviable DC and phagocytes that have taken up the tracking agent were imaged. Moreover, migration may be overestimated because therapeutic cells and phagocytes containing the tracking label cannot be distinguished by *in vivo* imaging. Thus, depending on the method of administration and the nature of the vaccine, immunohistochemical analysis of target organs will still be decisive for quantitative and qualitative evaluation of the efficacy of cellular therapy.

I.d. administration of DC vaccines is not only attractive for imaging purposes, it is also easier to do, and less time-consuming and less expensive than i.n. injection, which needs to be done under ultrasound guidance by an experienced radiologist. We found that after i.d. injection, never >4% of DC migrated to the draining lymph node, whereas up to 56% of the DC redistributed to distinct lymph nodes after i.n. injection. Despite these major differences in migrating DC, immunologic responses were comparable after both i.n. and i.d. DC injection. Up till now, the minimal amount of DC that is needed to induce an efficient immune response in humans is unknown. From our data, we can calculate that after i.d. injection, $<5 \times 10^5$ DC reach the T-cell area (in the case of a maximal migration of 4%, of which 84% accounts for viable DC after injection of 15×10^6 DC). Apparently, this low number of DC is sufficient to induce *de novo* immune responses. It is interesting that after four vaccinations, immune responses after i.n. injection of DC were not significantly higher than after i.d.

injection even though at least 10-fold to 30-fold more $SPIO^+$ cells reach the paracortex with each vaccination. An important difference is that after i.d. injection, only few macrophages migrate from the injection site into the lymph nodes, whereas after i.n. injection all macrophages are already inside. The presence of macrophages that have phagocytosed ^{111}In/SPIO DC in the paracortex ($\sim$50% of $SPIO^+$ cells after i.n. injection versus 13% after i.d. injection) may have a negative effect on the immune response; for instance, by the secretion of anti-inflammatory cytokines. CD163 was found to be exclusively expressed by anti-inflammatory (mφ2) and not by proinflammatory macrophage (mφ1) subsets cultured from monocytes (25). These mφ2 macrophages can induce regulatory T cells via the expression of membrane-bound tumor growth factor-β (26). Thus, the presence of large numbers of $CD163^+SPIO^+$ macrophages may dampen the immune response induced by the ^{111}In/SPIO DC.

Although we detected anti-KLH immune responses in most patients, TAA-specific immune responses were observed less frequently. One of the reasons may be the absence of MHC class II–restricted peptides. Also, the threshold for the activation of T cells specific for TAA tyrosinase and gp100 is likely higher than for the immunogenic foreign antigen KLH. Most importantly, the binding of exogenous-loaded TAA peptides to DC is not stable, and peptides may therefore be presented by fewer cells at lower densities and for a shorter period of time (27). An alternative way of antigen delivery would be loading of DC with antigens that need to be intracellularly processed. The use of antigens requiring processing results in prolonged antigen presentation (27), thereby increasing the time span during which the DC can activate specific T cells. Furthermore, DC may amplify the response by the transfer of antigen to resident DC in addition to presenting processed antigen to T cells themselves (28, 29). Increasing antigen presentation, immune stimulatory potential, and migratory capacities of DC for immunotherapy may greatly enhance the efficacy of DC therapy (reviewed in ref. 30). At present, we are comparing peptide-loaded DC with DC loaded with mRNA encoding for TAA. Initial findings show that when DC electroporated with TAA mRNA are injected into a lymph node, TAA protein expression was detectable up until 24 hours after injection.[10] Simultaneously, our research focuses on the generation of DC with high immune stimulatory capacity (31) and on maximizing migratory capacities and vaccine delivery. In addition, it will be worthwhile to investigate whether the injection of no more than 5×10^6 DC directly into a lymph node will already be sufficient to induce immunologic responses, as this will greatly reduce the need for large-scale production of DC and may make the use of DC that circulate in small numbers in the peripheral blood feasible. Optimizing both the generation of high migratory and immune stimulatory DC, and improving application and treatment strategies will be necessary to enhance the number of responding patients and advance experimental DC immune therapy into a standard treatment.

[10] Schuurhuis et al. submitted.

Disclosure of Potential Conflicts of Interest

No potential conflicts of interest were disclosed.

Acknowledgments

We thank Mandy van de Rakt, Marieke Kerkhoff, Nicole Scharenborg, Annemiek de Boer, Cathy Maass, Jos Rijntjes, Sandra Croockewit, Frank Preijers, Paul Ruijs, Christel van Riel, Maichel van Riel, and Wim van den Broek for their assistance and technical support.

References

1. Figdor CG, de Vries IJ, Lesterhuis WJ, Melief CJ. Dendritic cell immunotherapy: mapping the way. Nat Med 2004;10:475–80.
2. Nencioni A, Grunebach F, Schmidt SM, et al. The use of dendritic cells in cancer immunotherapy. Crit Rev Oncol Hematol 2008;65:191–9.
3. Lesterhuis WJ, Aarntzen EH, de Vries IJ, et al. Dendritic cell vaccines in melanoma: from promise to proof? Crit Rev Oncol Hematol 2008;66:118–34.
4. Eggert AA, Schreurs MW, Boerman OC, et al. Biodistribution and vaccine efficiency of murine dendritic cells are dependent on the route of administration. Cancer Res 1999;59:3340–5.
5. Okada N, Tsujino M, Hagiwara Y, et al. Administration route-dependent vaccine efficiency of murine dendritic cells pulsed with antigens. Br J Cancer 2001;84:1564–70.
6. Mullins DW, Sheasley SL, Ream RM, Bullock TN, Fu YX, Engelhard VH. Route of immunization with peptide-pulsed dendritic cells controls the distribution of memory and effector T cells in lymphoid tissues and determines the pattern of regional tumor control. J Exp Med 2003;198:1023–34.
7. Dudda JC, Simon JC, Martin S. Dendritic cell immunization route determines CD8+ T cell trafficking to inflamed skin: role for tissue microenvironment and dendritic cells in establishment of T cell-homing subsets. J Immunol 2004;172:857–63.
8. Mora JR, Bono MR, Manjunath N, et al. Selective imprinting of gut-homing T cells by Peyer's patch dendritic cells. Nature 2003;424:88–93.
9. de Vries IJ, Krooshoop DJ, Scharenborg NM, et al. Effective migration of antigen-pulsed dendritic cells to lymph nodes in melanoma patients is determined by their maturation state. Cancer Res 2003;63:12–7.
10. Morse MA, Coleman RE, Akabani G, Niehaus N, Coleman D, Lyerly HK. Migration of human dendritic cells after injection in patients with metastatic malignancies. Cancer Res 1999;59:56–8.
11. Quillien V, Moisan A, Carsin A, et al. Biodistribution of radiolabelled human dendritic cells injected by various routes. Eur J Nucl Med Mol Imaging 2005;32:731–41.
12. Ridolfi R, Riccobon A, Galassi R, et al. Evaluation of *in vivo* labelled dendritic cell migration in cancer patients. J Transl Med 2004;2:27.
13. Blocklet D, Toungouz M, Kiss R, et al. 111In-oxine and 99mTc-HMPAO labelling of antigen-loaded dendritic cells: *in vivo* imaging and influence on motility and actin content. Eur J Nucl Med Mol Imaging 2003;30:440–7.
14. Nair S, McLaughlin C, Weizer A, et al. Injection of immature dendritic cells into adjuvant-treated skin obviates the need for *ex vivo* maturation. J Immunol 2003;171:6275–82.
15. Thompson M, Wall DM, Hicks RJ, Prince HM. *In vivo* tracking for cell therapies. Q J Nucl Med Mol Imaging 2005;49:339–48.
16. Trakatelli M, Toungouz M, Blocklet D, et al. A new dendritic cell vaccine generated with interleukin-3 and interferon-β induces CD8+ T cell responses against NA17-2 tumor peptide in melanoma patients. Cancer Immunol Immunother 2006;55:469–74.
17. de Vries IJ, Lesterhuis WJ, Barentsz JO, et al. Magnetic resonance tracking of dendritic cells in melanoma patients for monitoring of cellular therapy. Nat Biotechnol 2005;23:1407–13.
18. Mackensen A, Krause T, Blum U, Uhrmeister P, Mertelsmann R, Lindemann A. Homing of intravenously and intralymphatically injected human dendritic cells generated *in vitro* from CD34+ hematopoietic progenitor cells. Cancer Immunol Immunother 1999;48:118–22.
19. Balch CM, Buzaid AC, Soong SJ, et al. Final version of the American Joint Committee on Cancer staging system for cutaneous melanoma. J Clin Oncol 2001;19:3635–48.
20. de Vries IJ, Eggert AA, Scharenborg NM, et al. Phenotypical and functional characterization of clinical grade dendritic cells. J Immunother 2002;25:429–38.
21. Thurner B, Haendle I, Roder C, et al. Vaccination with mage-3A1 peptide-pulsed mature, monocyte-derived dendritic cells expands specific cytotoxic T cells and induces regression of some metastases in advanced stage IV melanoma. J Exp Med 1999;190:1669–78.
22. Holtl L, Rieser C, Papesh C, et al. Cellular and humoral immune responses in patients with metastatic renal cell carcinoma after vaccination with antigen pulsed dendritic cells. J Urol 1999;161:777–82.
23. Vakkila J, Lotze MT, Riga C, Jaffe R. A basis for distinguishing cultured dendritic cells and macrophages

in cytospins and fixed sections. Pediatr Dev Pathol 2005;8:43–51.

24. de Vries IJ, Bernsen MR, Lesterhuis WJ, et al. Immunomonitoring tumor-specific T cells in delayed-type hypersensitivity skin biopsies after dendritic cell vaccination correlates with clinical outcome. J Clin Oncol 2005;23:5779–87.

25. Verreck FA, de Boer T, Langenberg DM, van der ZL, Ottenhoff TH. Phenotypic and functional profiling of human proinflammatory type-1 and anti-inflammatory type-2 macrophages in response to microbial antigens and IFN-γ- and CD40L-mediated costimulation. J Leukoc Biol 2006;79:285–93.

26. Savage ND, de Boer T, Walburg KV, et al. Human anti-inflammatory macrophages induce Foxp3+ GITR+ CD25+ regulatory T cells, which suppress via membrane-bound TGFβ-1. J Immunol 2008;181:2220–6.

27. Schnurr M, Chen Q, Shin A, et al. Tumor antigen processing and presentation depend critically on dendritic cell type and the mode of antigen delivery. Blood 2005;105:2465–72.

28. Allan RS, Waithman J, Bedoui S, et al. Migratory dendritic cells transfer antigen to a lymph node-resident dendritic cell population for efficient CTL priming. Immunity 2006;25:153–62.

29. Kleindienst P, Brocker T. Endogenous dendritic cells are required for amplification of T cell responses induced by dendritic cell vaccines *in vivo*. J Immunol 2003;170:2817–23.

30. Verdijk P, Aarntzen EH, Punt CJ, de Vries IJ, Figdor CG. Maximizing dendritic cell migration for cancer immunotherapy. Expert Opin Biol Ther 2008;8:865–74.

31. Boullart ACI, Aarntzen EH, Verdijk P, et al. Maturation of monocyte-derived dendritic cells with Toll-like receptor 3 and 7/8 ligands combined with prostaglandin E2 results in high interleukin-12 production and cell migration. Cancer Immunol Immunother 2008;57:1589–97.